Neutrino-neutrino scattering and matter-enhanced neutrino flavor transformation in supernovae

Yong-Zhong Qian and George M. Fuller*
Institute for Nuclear Theory, NK-12, University of Washington, Seattle, Washington 98195
(Received 30 June 1994; revised manuscript received 3 November 1994)

We examine matter-enhanced neutrino flavor transformation ($\nu_{\tau(\mu)} \rightleftharpoons \nu_e$) in the region above the neutrino sphere in type II supernovae. Our treatment explicitly includes contributions to the neutrino-propagation Hamiltonian from neutrino-neutrino forward scattering. A proper inclusion of these contributions shows that they have a completely negligible effect on the range of the ν_e-$\nu_{\tau(\mu)}$ vacuum mass-squared difference δm^2 and vacuum mixing angle θ or equivalently $\sin^2 2\theta$, required for enhanced supernova shock reheating. When neutrino background effects are included, we find that r-process nucleosynthesis from neutrino-heated supernova ejecta remains a sensitive probe of the mixing between a light ν_e and a $\nu_{\tau(\mu)}$ with a cosmologically significant mass. Neutrino-neutrino scattering contributions are found to have a generally small effect on the (δm^2, $\sin^2 2\theta$) parameter region probed by r-process nucleosynthesis. We point out that the nonlinear effects of the neutrino background extend the range of sensitivity of r-process nucleosynthesis to smaller values of δm^2.

PACS number(s): 14.60.Pq, 12.15.Ff, 97.10.Cv, 97.60.Bw

I. INTRODUCTION

In this paper we investigate the problem of matter-enhanced neutrino flavor transformation in the region above the neutrino sphere in type II supernovae. In particular, we examine the role of contributions to the neutrino-propagation Hamiltonian from neutrino-neutrino forward scattering. A general framework for treating these contributions in the context of the Mikeheyev-Smirnov-Wolfenstein (MSW) neutrino flavor transformation process has been given in Ref. [1]. (See Ref. [2] for a numerical study of the case of a pure neutrino gas.) Although the role of neutrino-neutrino scattering in the problem of matter-enhanced neutrino flavor conversion in supernovae has been treated previously [3,4], the present paper gives the first complete treatment utilizing the scheme of Ref. [1].

Recent studies have examined the MSW transformation of ν_τ or ν_μ into ν_e in the region above the neutrino sphere in the post-core-bounce supernova environment [5,6]. These studies suggest that if ν_τ or ν_μ has a mass in the cosmologically interesting range of 1–100 eV, then the matter-enhanced transformation $\nu_{\tau(\mu)} \rightleftarrows \nu_e$ will be possible in this region. Such a transformation can result in significant effects on supernova dynamics and/or nucleosynthesis.

If we define, for example, $|\nu_e\rangle$ and $|\nu_\tau\rangle$ to be flavor eigenstates of ν_e and ν_τ, and $|\nu_1\rangle$ and $|\nu_2\rangle$ to be the associated mass eigenstates, then the vacuum mixing angle θ is defined through

$$|\nu_e\rangle = \cos\theta|\nu_1\rangle + \sin\theta|\nu_2\rangle \ , \tag{1a}$$

$$|\nu_\tau\rangle = -\sin\theta|\nu_1\rangle + \cos\theta|\nu_2\rangle \ . \tag{1b}$$

Reference [5] shows that $\nu_{\tau(\mu)} \rightleftharpoons \nu_e$ mixing with $\sin^2 2\theta \gtrsim 10^{-7}$ in the region above the neutrino sphere at a few hundred milliseconds after the bounce of the core can result in a 30–60 % increase in the supernova shock energy. Reference [6] shows that the heavy element nucleosynthesis from the hot bubble region is sensitive to $\nu_{\tau(\mu)} \rightleftharpoons \nu_e$ mixing at a level of $\sin^2 2\theta \sim 10^{-5}$. This hot bubble region forms above the neutrino sphere ~ 3 sec after core bounce. These effects are sensitive to mixing angles far smaller than those which can be probed in laboratory experiments. These supernova effects ultimately may represent our most sensitive probe of putative neutrino dark matter.

However, studies [5] and [6] neglected the off-diagonal contributions of neutrino-neutrino scattering to the flavor-basis neutrino-propagation Hamiltonian. In what follows, we present a detailed study of neutrino flavor transformation in the post-core-bounce supernova environment. Our calculations include all effects of the neutrino background. We have adopted the overall principles and techniques of Ref. [1] in our treatment of neutrino-neutrino and neutrino-electron scattering contributions to the neutrino-propagation Hamiltonian. We find that neutrino background contributions have a negligible effect on the range of the ν_e-$\nu_{\tau(\mu)}$ vacuum mass-squared difference δm^2 and vacuum mixing angle θ (or $\sin^2 2\theta$) required for enhanced supernova shock reheating. A proper treatment of the ensemble average over the neutrino background shows that r-process nucleosynthesis from neutrino-heated supernova ejecta remains a sensitive probe of the mixing between a light ν_e and a ν_τ (or ν_μ) with a cosmologically significant mass ($m_{\nu_{\tau(\mu)}} \approx 1$–100 eV).

In Sec. II we discuss a general framework for treating

*Permanent address: Department of Physics, University of California, San Diego, La Jolla, CA 92093-0319.

neutrino flavor transformation in the supernova environment. In Sec. III we compute neutrino flavor transformation probabilities as functions of δm^2 and $\sin^2 2\theta$ relevant for the shock reheating and hot bubble r-process nucleosynthesis epochs of the supernova. We give conclusions in Sec. IV.

II. THE NEUTRINO-PROPAGATION HAMILTONIAN IN SUPERNOVAE

The general problem of the time evolution of the full density matrix for an ensemble of three flavors of neutrinos and antineutrinos with electron and positron backgrounds and a nucleon background is a daunting one. Several formal approaches to this problem have been made (cf. Ref. [1] and references therein). In the present paper, we shall only summarize the salient features of this previous work and tailor our subsequent discussion to the particular problem of neutrino propagation and flavor transformation in the region of the supernova environment above the neutrino sphere. Considerable simplification of the problem can be realized in this case.

The general time evolution of the neutrino density matrix ρ can be summarized as

$$i\dot{\rho} = [H, \rho] \ , \tag{2}$$

where $\rho = \sum_{jk} \rho_{jk} |j\rangle\langle k|$, $\dot{\rho} = d\rho/dt$, and j and k refer to all neutrino quantum numbers including momentum (energy), flavor, helicity, charge conjugation eigenvalue, etc. In Eq. (2), H is the full Schrödinger picture Hamiltonian including all neutrino self-interactions as well as interactions with the $e^{\pm}$ and nucleon backgrounds.

Without loss of generality we can follow a particular momentum component of Eq. (2) (cf. Ref. [1]), or equivalently, the associated Schrödinger equation for the time evolution of neutrino field amplitudes for a given momentum. The Hamiltonian operator in this case would have the dimensionality of the density matrix for the single momentum state (e.g., 12×12 for three Dirac neutrino flavors, since each neutrino state has either right-handed or left-handed helicity, and is either a neutrino or an antineutrino).

We argue that further simplification of this problem can be made through approximations motivated by the *particular* distribution functions for $\nu_e, \bar{\nu}_e, \nu_\mu, \bar{\nu}_\mu, \nu_\tau$, and $\bar{\nu}_\tau$ which obtain in the region above the neutrino sphere in the post-core-bounce epoch of type II supernovae. Since the distribution functions for $\nu_\mu, \bar{\nu}_\mu, \nu_\tau$, and $\bar{\nu}_\tau$ are all expected to be essentially identical, mixings between neutrinos in this sector will have no effect on any aspect of supernova physics. In other words, we need only consider mixings between ν_e and either ν_μ or ν_τ. If, as seems likely, the vacuum mass heirarchy for neutrinos satisfies $m_{\nu_{\tau(\mu)}} > m_{\nu_e}$, then we need only consider matter-enhanced mixing among neutrinos, as antineutrino mixing is suppressed by matter effects. On the other hand, if $m_{\nu_e} > m_{\nu_{\tau(\mu)}}$, then mixing in the neutrino sector is suppressed, and mixing in the antineutrino sector can be enhanced. In what follows, for illustrative purposes, we will consider the case where $\nu_{\tau(\mu)}$ is the heavier neutrino species. Our results can be generalized for the case of matter-enhanced antineutrino flavor transformation in obvious fashion.

The masses $m_{\nu_{\tau(\mu)}} \approx 1$–$100$ eV of interest in the post-core-bounce supernova environment are very small compared to the typical neutrino energies (average neutrino energy $\langle E_\nu \rangle$ is about or greater than 10 MeV). In this case we can neglect the population of right-handed Dirac neutrinos and left-handed Dirac antineutrinos produced by scattering processes. This is because helicity-flipping rates are proportional to $(m_\nu/E_\nu)^2$.

Taking advantage of these features allows us to reduce the dimensionality of the Hamiltonian in Eq. (2) to 2×2 for the Dirac neutrino case. If neutrinos are Majorana particles, then we have only left-handed neutrinos and right-handed antineutrinos, and again the Hamiltonian of interest is 2×2.

In any case, the neutrinos of interest in supernovae will be extremely relativistic, so that we can approximate the neutrino energy as $E_\nu = \sqrt{p^2 + m^2} \approx p + m^2/2p$. The first term in this expression, p, the momentum, just gives an overall phase to the coherent propagating neutrino state and can be ignored without loss of generality. The second term $m^2/2p$ is responsible for the relevant neutrino mixing behavior. The part of the Hamiltonian corresponding to the $m^2/2p$ term in vacuum, H_v, can be written in the flavor basis (e.g., $|\nu_e\rangle, |\nu_\tau\rangle$) as

$$H_v = \frac{\Delta}{2} \begin{pmatrix} -\cos 2\theta & \sin 2\theta \\ \sin 2\theta & \cos 2\theta \end{pmatrix} , \tag{3}$$

where θ is the vacuum mixing angle as in Eq. (1), $\Delta = \delta m^2/2E_\nu$, and $\delta m^2 \equiv m_2^2 - m_1^2$, with m_1 and m_2 the vacuum mass eigenvalues corresponding to the mass eigenstates $|\nu_1\rangle$ and $|\nu_2\rangle$, respectively.

In matter the relation between the flavor basis and the mass basis can be written as in Eq. (1), but with the vacuum mixing angle replaced by an appropriate matter mixing angle θ_n. For illustrative purposes consider the case where the only contribution to the effective mass difference between neutrino flavors comes from charged-current exchange scattering on electrons. We take the net number density of electrons to be

$$n_e \equiv n_{e^-} - n_{e^+} \ , \tag{4a}$$

where n_{e^-} (n_{e^+}) is the total proper number density of negatrons (positrons). The electron fraction Y_e is defined in terms of the total baryon rest mass density ρ_B and Avogardro's number N_A by

$$n_e = \rho_B Y_e N_A \ . \tag{4b}$$

The contribution to the Hamiltonian from neutrino-electron exchange scattering is

$$A = \sqrt{2} G_F n_e \ , \tag{5}$$

where G_F is the Fermi constant. In Fig. 1 we show a generic Feynman graph for ν_e-e scattering. To obtain the result in Eq. (5) one must sum graphs for ν_e-e^- and ν_e-e^+ scattering over the appropriate $e^{\pm}$ distribution functions. In this case the neutrino-propagation Hamiltonian H_e can be written as

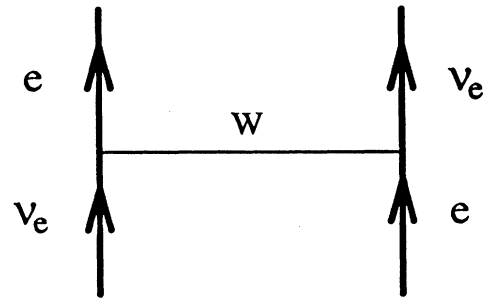

FIG. 1. A generic Feynman graph for ν_e-e scattering.

$$H_e = \frac{\Delta_{\rm eff}}{2}\begin{pmatrix} -\cos 2\theta_n & \sin 2\theta_n \\ \sin 2\theta_n & \cos 2\theta_n \end{pmatrix} = \frac{1}{2}\begin{pmatrix} -\Delta\cos 2\theta + A & \Delta\sin 2\theta \\ \Delta\sin 2\theta & \Delta\cos 2\theta - A \end{pmatrix}, \quad (6)$$

where $\Delta_{\rm eff} = \sqrt{(\Delta\cos 2\theta - A)^2 + \Delta^2\sin^2 2\theta}$. In these expressions the matter mixing angle θ_n is related to the vacuum mixing angle θ and the local net electron number density through

$$\sin 2\theta_n = \frac{\Delta\sin 2\theta}{\sqrt{(\Delta\cos 2\theta - A)^2 + \Delta^2\sin^2 2\theta}}, \quad (7a)$$

$$\cos 2\theta_n = \frac{\Delta\cos 2\theta - A}{\sqrt{(\Delta\cos 2\theta - A)^2 + \Delta^2\sin^2 2\theta}}. \quad (7b)$$

The amplitudes for antineutrino-electron ($\bar{\nu}_e$-e) forward exchange scattering and neutrino-electron (ν_e-e) forward exchange scattering have opposite signs. This implies that $\bar{\nu}_e$-e exchange scattering gives a contribution $-A$ to the flavor-basis interaction Hamiltonian for $\bar{\nu}_e$. In this case the matter mixing angle for antineutrinos, $\bar{\theta}_n$, satisfies

$$\sin 2\bar{\theta}_n = \frac{\Delta\sin 2\theta}{\sqrt{(\Delta\cos 2\theta + A)^2 + \Delta^2\sin^2 2\theta}}, \quad (8a)$$

$$\cos 2\bar{\theta}_n = \frac{\Delta\cos 2\theta + A}{\sqrt{(\Delta\cos 2\theta + A)^2 + \Delta^2\sin^2 2\theta}}. \quad (8b)$$

We note that the vacuum mixing angles for the neutrino and antineutrino sectors are the same.

On the assumption that $m_2 > m_1$ and $\theta < \pi/4$ (i.e., $\nu_{\tau(\mu)}$ is the heavier neutrino species), it is evident from Eqs. (7a) and (7b) that matter effects can give enhancement of flavor mixing in the neutrino sector. Mixing is maximal at a mass level crossing, or resonance, where $\Delta\cos 2\theta = A$ [7]. On the other hand, Eqs. (8a) and (8b) show that matter effects give a suppression of flavor mixing in the antineutrino sector. However, if $\nu_{\tau(\mu)}$ is lighter than ν_e (e.g., $m_2 > m_1$ but $\pi/4 < \theta < \pi/2$), the situation is reversed. In that case, mixing in the neutrino sector is suppressed, while mixing in the antineutrino sector can be enhanced.

In the supernova environment, however, the neutrino background and the resultant neutrino-neutrino forward exchange-scattering effects necessitate some modification of the above treatment of neutrino flavor transformation. In the region above the neutrino sphere in post-core-bounce type II supernovae the neutrino fluxes can be sizable (see, for example, the discussion in Ref. [6]). Individual neutrinos emitted from the neutrino sphere can be described as coherent states. However, each emitted neutrino is related to every other emitted neutrino in an incoherent fashion. In other words, these different individual (or single) neutrino states have random relative phases, as is characteristic of a thermal emission process. The total neutrino field is properly a *mixed* ensemble of individual neutrino states. It is not a coherent many-body state. Accordingly, the total neutrino density matrix is an incoherent sum over each *single* neutrino density matrix.

For a single neutrino emitted at the neutrino sphere as a ν_α (e.g., in flavor state $\alpha = e, \tau$ for the case of two-neutrino mixing) we can represent its state at some point above the neutrino sphere as

$$|\psi_{\nu_\alpha}\rangle = a_{1\alpha}(t)|\nu_1(t)\rangle + a_{2\alpha}(t)|\nu_2(t)\rangle, \quad (9)$$

where $|\nu_1(t)\rangle$ and $|\nu_2(t)\rangle$ are the instantaneous physical mass eigenstates of the full neutrino-propagation Hamiltonian, and $a_{1\alpha}(t)$ and $a_{2\alpha}(t)$ are the corresponding complex amplitudes. Normalization requires that we take $|a_{1\alpha}(t)|^2 + |a_{2\alpha}(t)|^2 = 1$. In these expressions the time t could be any evolutionary parameter (e.g., density, radius, etc.) along the neutrino's path from its creation position at the neutrino sphere to a point at radius r. The single neutrino density matrix is then given by

$$|\psi_{\nu_\alpha}\rangle\langle\psi_{\nu_\alpha}| = |a_{1\alpha}(t)|^2|\nu_1(t)\rangle\langle\nu_1(t)| + |a_{2\alpha}(t)|^2|\nu_2(t)\rangle\langle\nu_2(t)| + a^*_{1\alpha}(t)a_{2\alpha}(t)|\nu_2(t)\rangle\langle\nu_1(t)| + a_{1\alpha}(t)a^*_{2\alpha}(t)|\nu_1(t)\rangle\langle\nu_2(t)|. \quad (10)$$

The density matrix representing the mixed ensemble of single neutrino states all with momentum $\mathbf{p}$ can be written as the incoherent sum

$$\rho_{\mathbf{p}} d^3\mathbf{p} = \sum_\alpha dn_{\nu_\alpha}|\psi_{\nu_\alpha}\rangle\langle\psi_{\nu_\alpha}|. \quad (11)$$

In this expression the sum runs over, for example, $\alpha = e, \tau$, while dn_{ν_α} is the local differential number density of ν_α neutrinos with momentum $\mathbf{p}$ in interval $d^3\mathbf{p}$. The local differential ν_α neutrino number density at a point at radius r above a neutrino sphere with radius R_ν is

$$dn_{\nu_\alpha} \approx n^0_{\nu_\alpha} f_{\nu_\alpha}(E_{\nu_\alpha}) dE_{\nu_\alpha}\left(\frac{d\Omega_{\mathbf{p}}}{4\pi}\right), \quad (12a)$$

where $d\Omega_{\mathbf{p}}$ is the differential solid angle (pencil of direc-

tions) along the neutrino momentum $\mathbf{p}$ ($|\mathbf{p}| \approx E_{\nu_\alpha}$), $n^0_{\nu_\alpha}$ is the ν_α neutrino number density at the neutrino sphere, and $f_{\nu_\alpha}(E_{\nu_\alpha})$ is the normalized ν_α energy distribution function. We can show [6] that a good approximation for $n^0_{\nu_\alpha}$ is

$$n^0_{\nu_\alpha} \approx \frac{L_{\nu_\alpha}}{\langle E_{\nu_\alpha}\rangle}\frac{1}{\pi R_\nu^2 c} , \tag{12b}$$

where L_{ν_α} is the luminosity in ν_α neutrinos, $\langle E_{\nu_\alpha}\rangle$ is the average ν_α neutrino energy, and c is the speed of light. The normalized ν_α neutrino energy distribution function can be well approximated by

$$f_{\nu_\alpha}(E_{\nu_\alpha}) \approx \frac{1}{F_2(0)}\frac{1}{T^3_{\nu_\alpha}}\frac{E^2_{\nu_\alpha}}{\exp(E_{\nu_\alpha}/T_{\nu_\alpha})+1} , \tag{12c}$$

where the rank 2 Fermi integral with argument zero is $F_2(0) \approx 1.803$, and where T_{ν_α} is the ν_α neutrino sphere temperature. The average ν_α neutrino energy is related to the appropriate neutrino sphere temperature by $\langle E_{\nu_\alpha}\rangle \approx 3.15 T_{\nu_\alpha}$.

In the region of the supernova above the neutrino sphere, the range of the solid angle contribution allowed in Eq. (12a) is restricted to be within the solid angle subtended by the neutrino sphere as seen from a point at radius r. The geometrical arrangement of a neutrino sphere with radius R_ν, a point above the neutrino sphere at radius r, and various neutrino paths are depicted in Fig. 2. We can now write the full flavor-basis neutrino-propagation Hamiltonian as a sum of vacuum mass and electron background contributions H_e and neutrino background contributions $H_{\nu\nu}$:

$$H = H_e + H_{\nu\nu} , \tag{13a}$$

where $H_{\nu\nu}$ represents the ensemble average over neutrino-neutrino interactions using the density matrix in Eq. (11). For a neutrino with energy E_ν and momentum $\mathbf{p}$ propagating radially outside the neutrino sphere we can write

$$H_{\nu\nu} = \sqrt{2}G_F \int (1-\cos\theta_{\mathbf{q}})(\rho_{\mathbf{q}} - \bar\rho_{\mathbf{q}})d^3\mathbf{q} , \tag{13b}$$

where $\bar\rho_{\mathbf{q}}$ is the density matrix for antineutrinos with momentum $\mathbf{q}$ [defined in obvious analogy to $\rho_{\mathbf{p}}$ in Eq. (11)] and $\theta_{\mathbf{q}}$ is the angle between the direction of the propagating neutrino with momentum $\mathbf{p}$ and the directions of other neutrinos in the ensemble with momentum $\mathbf{q}$. We can generalize the expression for $H_{\nu\nu}$ in Eq. (13b) for nonradially propagating neutrinos by replacing $\cos\theta_{\mathbf{q}}$ with $\mathbf{q}\cdot\mathbf{p}/\{|\mathbf{q}||\mathbf{p}|\}$.

It is convenient to recast Eq. (13b) in the form

$$H_{\nu\nu} = \frac{1}{2}\begin{pmatrix} B & B_{e\tau} \\ B_{\tau e} & -B \end{pmatrix} + \frac{\sqrt{2}}{2}G_F \int (1-\cos\theta_{\mathbf{q}})\mathrm{Tr}(\rho_{\mathbf{q}} - \bar\rho_{\mathbf{q}})d^3\mathbf{q} . \tag{14}$$

Note that the second term in this equation is simply proportional to the identity matrix, implying that it provides only an overall phase in the propagating neutrino state and can be ignored.

In the first term in Eq. (14) there are two contributions to the neutrino-propagation Hamiltonian, B and $B_{e\tau}(B_{\tau e})$, where

$$B = \sqrt{2}G_F \int (1-\cos\theta_{\mathbf{q}})[(\rho_{\mathbf{q}} - \bar\rho_{\mathbf{q}})_{ee} - (\rho_{\mathbf{q}} - \bar\rho_{\mathbf{q}})_{\tau\tau}]d^3\mathbf{q} , \tag{15a}$$

$$B_{e\tau} = 2\sqrt{2}G_F \int (1-\cos\theta_{\mathbf{q}})(\rho_{\mathbf{q}} - \bar\rho_{\mathbf{q}})_{e\tau}d^3\mathbf{q} , \tag{15b}$$

$$B_{\tau e} = 2\sqrt{2}G_F \int (1-\cos\theta_{\mathbf{q}})(\rho_{\mathbf{q}} - \bar\rho_{\mathbf{q}})_{\tau e}d^3\mathbf{q} , \tag{15c}$$

where, for example, by $(\rho_{\mathbf{q}})_{e\tau}$ we mean the matrix element of the density matrix operator, $\langle\nu_e|\rho_{\mathbf{q}}|\nu_\tau\rangle$, while by $(\bar\rho_{\mathbf{q}})_{e\tau}$ we mean $\langle\bar\nu_e|\rho_{\mathbf{q}}|\bar\nu_\tau\rangle$.

Here B corresponds to the forward neutrino-neutrino exchange-scattering contributions to the neutrino effective mass. These contributions are the analogues of the ν_e-e exchange-scattering term A in Eqs. (5) and (6). Generic Feynman graphs for these neutrino-neutrino exchange processes are shown in Fig. 3(a) for ν_e-ν_e scattering and in Fig. 3(b) for ν_τ-ν_τ scattering. We will later refer to B as the "diagonal" contribution of the neutrino background to the flavor-basis neutrino-propagation Hamiltonian.

The neutrino background also provides "off-diagonal" terms in the flavor-basis neutrino-propagation Hamiltonian. These are, for example, the $B_{e\tau}$ and $B_{\tau e}$ terms above. They arise because the background neutrinos are not in flavor eigenstates [1]. We show graphically these contributions for ν_e and ν_τ neutrinos with momenta $\mathbf{p}$ and $\mathbf{q}$ in Fig. 4. The corresponding diagonal and off-diagonal contributions to the flavor-basis antineutrino-

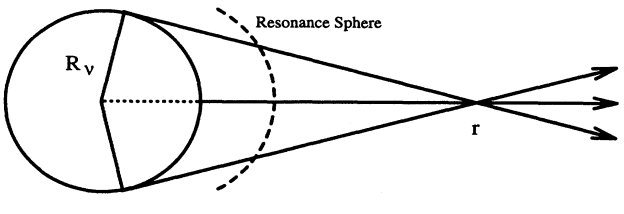

FIG. 2. The geometrical arrangement of a neutrino sphere with radius R_ν, a point above the neutrino sphere at radius r, and various neutrino paths. The dashed line in this figure represents the resonance sphere for neutrinos with a specific energy E_ν.

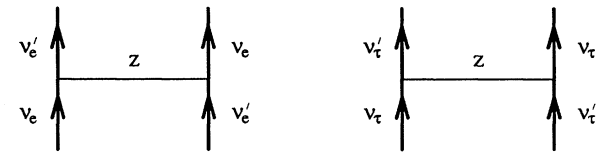

FIG. 3. Generic Feynman graphs for neutrino-neutrino exchange-scattering processes. (a) is for ν_e-ν_e scattering and (b) is for ν_τ-ν_τ scattering.

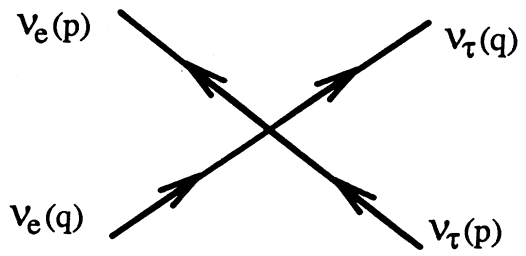

FIG. 4. Graphic representation for off-diagonal contributions from the neutrino background.

propagation Hamiltonian from the neutrino background are $-B$ and $-B_{e\tau}$ $(-B_{\tau e})$, respectively.

The evaluation of B and $B_{e\tau}$ $(B_{\tau e})$ is quite straightforward in the case where neutrino flavor evolution is adiabatic. This is because the cross terms in the neutrino density matrices can be taken to vanish in this case. For example, if we are interested in the flavor evolution history of an adiabatically evolving "test" neutrino which is resonant at energy E_R, then due to the nature of the density gradient in the post-core-bounce supernova environment, all background neutrinos with energies $E_\nu \leq E_R$ encountered by this test neutrino will evolve through *their* resonances adiabatically. The resonance positions for these background neutrinos will lie below that for the test neutrino with energy E_R. All neutrinos which have a specific energy E_ν will go through resonance on what we term their "resonance sphere." We show an example of a resonance sphere as a dashed line in Fig. 2. Background neutrinos with energies $E_\nu > E_R$ will not have gone through their resonances prior to reaching the resonance position for the test neutrino, so that we can regard their evolution as adiabatic in (and through) the resonance region for the test neutrino. Since the electron number density always dominates the effective neutrino number density in determining the weak potential near the neutrino sphere, and since the electron number density is always very large there ($n_e \sim 10^{35}$ cm^{-3}, cf. Refs. [5,6]), neutrinos leaving the neutrino sphere are well approximated as being in mass eigenstates. If, subsequently, their evolution is adiabatic, then we see immediately that the cross terms in the single neutrino density matrices [the last two terms in Eq. (10)] always vanish. Since antineutrinos do not go through resonance in supernovae, their evolution is always adiabatic, and the cross terms in the single antineutrino density matrices vanish accordingly.

The situation for nonadiabatic flavor evolution is more complex. Clearly, background neutrinos with energies $E_\nu > E_R$ can still be regarded as evolving adiabatically in the region below the resonance position corresponding to a neutrino with energy E_R. For this case, we can safely set the cross terms in the single neutrino density matrices to zero.

It is obvious, however, that background neutrinos with energies $E_\nu \leq E_R$ generally cannot be regarded as evolving adiabatically if the test neutrino with energy E_R evolves nonadiabatically through its resonance. Each background neutrino can be regarded as evolving adiabatically only in the region *below* its own resonance sphere. Once a neutrino propagates through its resonance position, both mass eigenstates are essentially "regenerated," and the ket for the neutrino state above this position is, in general, a linear combination of both mass eigenstates, as in Eq. (9). The relative phase between the two amplitudes in this linear combination begins developing (evolving) above the resonance sphere.

Adroit attention to the phases of the background neutrinos shows that phase averaging (in the ensemble average) results in vanishingly small cross terms in the corresponding single neutrino density matrices whenever the energies of the background neutrinos are sufficiently less than E_R. This phase-averaging reduction in the cross terms comes about from two mechanisms: (1) differences in the path lengths for background neutrinos of a given energy propagating from different positions on their resonance sphere to a point on the resonance sphere for the test neutrino with energy E_R, and (2) the fact that the background neutrinos contributing to the ensemble averages have a range of energies [cf. the distribution functions in Eqs. (12a)–(12c)].

Let us first consider the phase-averaging reduction in the cross terms in the single neutrino density matrix resulting from path length differences for background neutrinos of a given energy.

The last two terms in Eq. (10) are the cross terms. They have coefficients $a_1^*(t)a_2(t)$ and $a_1(t)a_2^*(t)$, respectively. Each cross term is proportional to a factor $\sim \exp[i\int \omega_{12}(t)dt]$, with ω_{12} the difference in the local neutrino flavor-oscillation frequencies of the two mass eigenstates $|\nu_1(t)\rangle$ and $|\nu_2(t)\rangle$. These oscillation frequencies are, in turn, dependent on the local density. In both the early post-core-bounce shock reheating epoch (time post-core-bounce $t_{\rm PB} \sim 0.1$–1s) and in the hot bubble r-process nucleosynthesis epoch ($t_{\rm PB} \sim 3$–15 s) the electron number density predominantly determines the neutrino flavor-oscillation frequency in the region just above the neutrino sphere [5,6]. This is because the net neutrino number densities are negligible compared to the electron number densities in this region [5,6]. The Hamiltonian H_e in Eq. (6) is by itself sufficient to determine the neutrino flavor-oscillation frequencies in this region. The local neutrino flavor-oscillation frequency difference in this case is $\omega_{12} \approx \Delta_{\rm eff} = \sqrt{(\Delta\cos 2\theta - A)^2 + \Delta^2 \sin^2 2\theta}$.

For regions further from the neutrino sphere the electron number density may not completely dominate the weak potential, but it certainly provides a major component (cf. Ref. [6]). In any case, the neutrino-neutrino forward scattering contribution to the weak potential is clearly also radius and position dependent. The cross terms in Eq. (10) will have position-varying oscillation frequencies resulting from both of these components of the weak potential.

However, for neutrinos propagating through regions above their resonance spheres, and considering just the electron contribution to the weak potential, we can approximate the local neutrino flavor-oscillation frequency as being close to its vacuum value $\omega_{12} \approx \Delta$. Of course, this is only strictly true for positions well away from res-

onance. For a background neutrino with energy E_ν this condition will be met over most of the path length from its resonance sphere to the point where it encounters a resonant test neutrino of energy E_R, so long as E_ν is sufficiently less than E_R. Clearly, this condition will break down when the resonance sphere for the background neutrino lies within the resonance width for the neutrino with energy E_R. In turn, this will occur when the background neutrino has an energy which lies in the range $E_R(1-\tan 2\theta)$ to E_R [cf. Eq. (7a)]. Let us begin by considering the effect of phase averaging on the contribution of background neutrinos to ensemble averages when they have energies which lie outside (below) this range.

When taking the ensemble average over the neutrino background we necessarily integrate $\rho_{\mathbf{q}}$ over neutrino momentum *directions* to a point at radius r. We thereby also average over the oscillating cross terms in Eq. (10). In addition, neutrinos with different momentum directions travel on paths with different lengths from the resonance sphere to arrive at a point at radius r. These different path lengths from the resonance sphere then give rise to different phases for the oscillating factor $\sim \exp[i\int \omega_{12}(t)dt]$ in the cross terms in Eq. (10). In fact, it is clear from Fig. 2 that each neutrino path from a resonance sphere to a point at radius r will have a path length which depends on the polar angle. For neutrinos with momentum magnitude $|\mathbf{q}|$ (and energy E_ν) each path with a different polar angle will have a different phase entering into the cross term coefficients of Eq. (10). The phase difference $\delta\phi$ corresponding to a path length difference δr between two different neutrino propagation directions is then

$$\delta\phi \approx \Delta\delta r = \frac{\delta m^2}{2E_\nu}\delta r \approx \left(\frac{\delta m^2}{eV^2}\right)\left(\frac{25\ \mathrm{MeV}}{E_\nu}\right)\left(\frac{\delta r}{10^3\ \mathrm{cm}}\right) . \tag{16a}$$

Path length differences of order 0.1 km give rise to phase differences of $\gg 2\pi$. In this case, when averaged over all neutrino momentum directions, it is obvious that the contributions of the cross terms in the single neutrino density matrix in Eq. (10) to ensemble averages of quantities would vanish. When this regime obtains, we could set the cross terms to zero with no appreciable loss of accuracy in the ensemble averages.

Note, however, that the largest path length difference will arise between a neutrino propagating radially to a point at radius r and one which propagates from the limb of the neutrino sphere to this point. If the resonance sphere for these neutrinos has radius R (where $R < r$), then the path length difference between these neutrinos would be

$$\begin{aligned}\delta r &= \sqrt{r^2 - R_\nu^2} - \sqrt{R^2 - R_\nu^2} - (r - R) \\ &\approx (R_\nu^2/2rR)(r - R) .\end{aligned} \tag{16b}$$

Here, as above, R_ν is the radius of the neutrino sphere. The resonance positions lie in the region where $r \lesssim 40$ km at $t_{\rm PB} > 1$s [6]. This implies that $R_\nu/r > 1/4$ [6], so that getting the requisite path length difference ($\delta r \gtrsim 0.1$ km) for effective phase-averaging reduction of the cross terms would require that $r - R \gtrsim 3$ km. Background neutrinos of a given energy which had a resonance sphere closer to position r than about 3 km would not have the cross terms in their density matrices significantly reduced by direction averaging. It turns out, however, that in this case we will find that the averaging over the energy distributions of neutrinos with a given direction is far more effective at reducing the cross term contributions to ensemble averages.

In the ensemble average for $B, B_{e\tau}$, and $B_{\tau e}$ implicit in Eqs. (15a)–(15c) it is evident that, for a given neutrino propagation direction, we will integrate the cross terms in Eq. (10) over the neutrino energy distribution functions [Eqs. (12a)–(12c)]. Consider the effect of integrating the cross terms over an interval in energy $E_R - \delta E$ to E_R where, as above, E_R represents the energy of a fiducial test neutrino. The position of the resonance sphere for a background neutrino of energy E_R is coincident with that for the test neutrino, whereas, a background neutrino with energy $E_R - \delta E$ will have a resonance position which lies below that for the test neutrino. If we designate the difference of the densities between the positions of the resonance spheres for these neutrinos of differing energy as δn, then the difference of the radii of the resonance spheres is roughly $\delta r \approx \mathcal{H}|\delta n/n|$. Here $\mathcal{H}$ is the density scale height (cf. Refs. [5,6]), which at $t_{\rm PB} \gtrsim 1$s ranges from about 0.5 km near the neutrino sphere to about 10 km near the resonance position for a 25 MeV neutrino with $\delta m^2 \approx 1$ eV^2. Because the resonance density is inversely proportional to neutrino energy for a given δm^2, we can conclude that $\delta r \approx \mathcal{H}|\delta n/n| \approx \mathcal{H}\delta E/E_R$.

In this example, neutrinos with energy close to E_R will not have built up any phase at the resonance position for E_R, which we designate $t_{\rm res}(E_R)$. In contrast, those neutrinos in the distribution with energies close to $E_R - \delta E$ will have built up a phase of order

$$\phi \approx \int_{t_{\rm res}(E_R - \delta E)}^{t_{\rm res}(E_R)} \Delta_{\rm eff} dt \approx \Delta\delta r , \tag{16c}$$

by the time they get to $t_{\rm res}(E_R)$. In this expression $t_{\rm res}(E_R - \delta E)$ denotes the resonance sphere position for a background neutrino with energy $E_R - \delta E$, and we have assumed this position is well separated from $t_{\rm res}(E_R)$. This is true when $\delta E \gg E_R \tan 2\theta$. In this case we can approximate $\Delta_{\rm eff}$ as the vacuum value, Δ, over most of the path length of this neutrino from its resonance sphere to $t_{\rm res}(E_R)$. The characteristic spread in the phases of the cross terms entering into ensemble averages at $t_{\rm res}(E_R)$ will be $\delta\phi \approx \phi$, and thus we can conclude that

$$\delta\phi \approx 80\left(\frac{\delta m^2}{\mathrm{eV}^2}\right)\left(\frac{\delta E}{\mathrm{MeV}}\right)\left(\frac{25\ \mathrm{MeV}}{E_R}\right)^2\left(\frac{\mathcal{H}}{10\ \mathrm{km}}\right) . \tag{16d}$$

It is clear from Eq. (16d) and the relevant supernova model parameters that averaging over a portion $\delta E \gtrsim 0.1$ MeV of the distribution function for background neutrinos will produce $\delta\phi \gtrsim 2\pi$ and, thus, result in negligible

net cross term effects in ensemble averages. Of course, a characteristic spread in neutrino energies encountered in averaging over the neutrino distribution functions will be of order the appropriate neutrino sphere temperature, $\delta E \sim T_\nu \gtrsim 4$ MeV. This characteristic energy spread is much greater than $E_R \tan 2\theta$ for the vacuum mixing angles we will consider.

However, one might question the effectiveness of phase averaging, since as we increase the spread in energies, δE, in the average, the neutrino occupation numbers at those energies vary. Note, however, that they vary relatively slowly, since the neutrino energies important for changing the electron fraction and affecting nucleosynthesis generally satisfy $E_\nu \gtrsim 25$ MeV. Further ameliorating the deleterious effects of changing occupation numbers on the effectiveness of phase averaging is the fact that the ensemble averages also include a sum over neutrino flavors. Different neutrino flavors have different characteristic neutrino sphere temperatures ($T_{\nu_e} \sim 4$ MeV, $T_{\nu_{\tau(\mu)}} \sim 8$ MeV), so that a small increment δE around $E_R \approx 25$ MeV sometimes produces small compensating changes in the neutrino occupation numbers. In fact, when all the above effects are taken into account, a typical energy spread of order $\delta E \sim 0.1$ MeV centered around $E_R \approx 25$ MeV will give very good phase-averaging reduction in the contributions from the cross terms in the single neutrino density matrix.

The above arguments lead us to conclude that one can neglect the cross terms in Eq. (10) for all background neutrino energies except for those in the narrow range $E_R(1 - \tan 2\theta)$ to $E_R(1 + \tan 2\theta)$ around the resonance position (defined by E_R) for our test neutrino. Background neutrinos with energies above this range can be regarded as evolving adiabatically and thus have zero cross terms, while those with energies below this range will have their cross terms effectively "reduced" by phase averaging. It is obvious from the neutrino distribution functions presented in Eqs. (12a)–(12c) that the number of neutrinos contained in the energy range $E_R(1-\tan 2\theta)$ to $E_R(1+\tan 2\theta)$ will be very small for the vacuum mixing angles for which nonadiabatic neutrino flavor transformation has important effects on supernova nucleosynthesis ($\sin^2 2\theta \lesssim 10^{-4}$).

To put this in perspective, a test neutrino at resonance encounters a neutrino background in its resonance region in which only of order one neutrino in a thousand brings appreciable cross terms into ensemble averages for B and $B_{e\tau}$ ($B_{\tau e}$). Most of the values of B and $B_{e\tau}$ ($B_{\tau e}$) at this position will be determined by neutrinos for which we can safely set the cross terms in Eq. (10) to zero. We argue below that the effects of retention of the cross term phases of this very small number of neutrinos on neutrino flavor evolution are negligible.

Based on these arguments, in what follows we will make an approximation and consider only the first two terms of Eq. (10) in evaluating matrix elements of the density matrices $\rho_{\mathbf{q}}$ and $\bar{\rho}_{\mathbf{q}}$ [cf. Eq. (11)]. This will allow considerable simplification in computation of B and $B_{e\tau}$ ($B_{\tau e}$) from Eqs. (15a)–(15c). This is, obviously, an excellent approximation for adiabatic neutrino flavor evolution. We must keep in mind, however, that our treatment of nonadiabatic neutrino flavor evolution will be approximate and will not account for the very small number of neutrinos for which cross term phases cannot be neglected in the computation of neutrino flavor transformation at resonance. Though we feel that such an approximation is reasonable, at least in so far as expected effects on supernova nucleosynthesis are concerned, we note that only a detailed numerical calculation in which the phases of neutrinos are followed through resonance regions will show the range of validity of our approximation for the nonadiabatic case. The purpose of this paper is to map out the expected effects of the neutrino background on neutrino flavor transformation in various venues in supernovae, and so we will leave the small effects of resonant background neutrinos to a later work.

Failure to account properly for phase averaging in the ensemble averages for B and $B_{e\tau}$ ($B_{\tau e}$) would result in unphysical effects from the cross terms in the neutrino density matrix elements, Eqs. (15a)–(15c). This would introduce a spurious, and unphysical, "coherence" from the neutrino background in any treatment of nonadiabatic neutrino flavor evolution. We contend that phase-averaging reduction of the cross term effects in the ensemble average over the neutrino background is a key point in determining nonadiabatic neutrino flavor evolution in the region above the neutrino sphere in supernovae. This point has not been previously emphasized. Of course, these cross terms rigorously vanish in the case of adiabatic neutrino flavor evolution.

Note that $B_{e\tau} = B_{\tau e}$ since the terms in the ensemble averages, Eqs. (15a)–(15c), are all real and the Hamiltonian must be Hermitian. We note, however, that these terms [Eqs. (15a)–(15c)] are, in general, always real only when the cross terms in the single neutrino density matrix elements are neglected. This is the approximation made in this work. The full flavor-basis Hamiltonian which includes both the electron and neutrino backgrounds is now

$$H = H_e + H_{\nu\nu} = \frac{1}{2}\begin{pmatrix} -\Delta\cos 2\theta + A + B & \Delta\sin 2\theta + B_{e\tau} \\ \Delta\sin 2\theta + B_{e\tau} & \Delta\cos 2\theta - A - B \end{pmatrix} . \quad (17a)$$

In analogy to the discussion preceding Eq. (6) we can rewrite this Hamiltonian as

$$H = \frac{\Delta_H}{2}\begin{pmatrix} -\cos 2\theta_H & \sin 2\theta_H \\ \sin 2\theta_H & \cos 2\theta_H \end{pmatrix} . \quad (17b)$$

In this expression we have defined a full effective mixing angle θ_H which, in analogy to Eq. (1), gives the relations between the flavor basis and the instantaneous mass basis including the effects of both the electron and neutrino backgrounds:

$$|\nu_e\rangle = \cos\theta_H(t)|\nu_1(t)\rangle + \sin\theta_H(t)|\nu_2(t)\rangle , \quad (18a)$$

$$|\nu_\tau\rangle = -\sin\theta_H(t)|\nu_1(t)\rangle + \cos\theta_H(t)|\nu_2(t)\rangle . \quad (18b)$$

We have defined Δ_H as

$$\Delta_H \equiv \sqrt{(\Delta\cos2\theta - A - B)^2 + (\Delta\sin2\theta + B_{e\tau})^2} \ . \quad (19)$$

The full effective mixing angle satisfies

$$\sin2\theta_H = \frac{\Delta\sin2\theta + B_{e\tau}}{\sqrt{(\Delta\cos2\theta - A - B)^2 + (\Delta\sin2\theta + B_{e\tau})^2}} \ , \quad (20a)$$

$$\cos2\theta_H = \frac{\Delta\cos2\theta - A - B}{\sqrt{(\Delta\cos2\theta - A - B)^2 + (\Delta\sin2\theta + B_{e\tau})^2}} \ . \quad (20b)$$

Note that in the absence of a neutrino background $\Delta_H = \Delta_{\rm eff}$ and $\theta_H = \theta_n$. The corresponding expressions for the full effective mixing angle $\bar{\theta}_H$ in the antineutrino sector are obtained by replacing A, B, and $B_{e\tau}$ with $-A$, $-B$, and $-B_{e\tau}$, respectively.

As discussed above, the cross terms in the single neutrino density matrix will be approximated here as giving no contribution to the ensemble averages. With this approximation, we can write a reduced expression for the single neutrino density matrix in terms of flavor-basis eigenbras and eigenkets:

$$(|\psi_{\nu_\alpha}\rangle\langle\psi_{\nu_\alpha}|)_{\rm reduced} = \left\{\frac{1}{2} - \left[\frac{1}{2} - |a_{1\alpha}(t)|^2\right]\cos2\theta_H(t)\right\}|\nu_e\rangle\langle\nu_e| + \left\{\frac{1}{2} + \left[\frac{1}{2} - |a_{1\alpha}(t)|^2\right]\cos2\theta_H(t)\right\}|\nu_\tau\rangle\langle\nu_\tau|$$
$$+ \left[\frac{1}{2} - |a_{1\alpha}(t)|^2\right]\sin2\theta_H(t)(|\nu_e\rangle\langle\nu_\tau| + |\nu_\tau\rangle\langle\nu_e|) \ . \quad (21)$$

We should note that without the approximation that the cross terms vanish, it would not be possible to write simple analytic expressions for the full effective mixing angle [Eqs. (20a) and (20b)] which would be valid everywhere.

With this form for the single neutrino density matrix, it is straightforward to evaluate flavor-basis matrix elements of the density matrix operator. For example, the expressions in Eqs. (15a)–(15c) become

$$B = -\sqrt{2}G_F \sum_\alpha \int (1 - \cos\theta_{\mathbf{q}})\{[1 - 2|a_{1\alpha}(t)|^2]\cos2\theta_H(t)dn_{\nu_\alpha} - [1 - 2|\bar{a}_{1\alpha}(t)|^2]\cos2\bar{\theta}_H(t)dn_{\bar{\nu}_\alpha}\} \ , \quad (22a)$$

$$B_{e\tau} = \sqrt{2}G_F \sum_\alpha \int (1 - \cos\theta_{\mathbf{q}})\{[1 - 2|a_{1\alpha}(t)|^2]\sin2\theta_H(t)dn_{\nu_\alpha} - [1 - 2|\bar{a}_{1\alpha}(t)|^2]\sin2\bar{\theta}_H(t)dn_{\bar{\nu}_\alpha}\} \ . \quad (22b)$$

In these expressions $a_{1\alpha}(t)$ is the amplitude to be in the instantaneous mass eigenstate $|\nu_1(t)\rangle$ for an individual neutrino of momentum $\mathbf{q}$ which was created at the neutrino sphere ($t = 0$) in flavor eigenstate $|\nu_\alpha\rangle$. Likewise, $\bar{a}_{1\alpha}(t)$ is the amplitude to be in the instantaneous mass eigenstate $|\bar{\nu}_1(t)\rangle$ for an antineutrino of momentum $\mathbf{q}$ created at the neutrino sphere in flavor eigenstate $|\bar{\nu}_\alpha\rangle$. The expressions dn_{ν_α} and $dn_{\bar{\nu}_\alpha}$ are as given in Eq. (12a), e.g., $dn_{\nu_\alpha} \approx n^0_{\nu_\alpha} f_{\nu_\alpha}(E_{\nu_\alpha})dE_{\nu_\alpha}(d\Omega_{\mathbf{q}}/4\pi)$.

It remains to evaluate these expressions for the particular conditions (electron number density run and neutrino distribution functions) which obtain for the shock reheating and hot bubble r-process nucleosynthesis epochs.

III. NEUTRINO FLAVOR TRANSFORMATION IN THE SUPERNOVA ENVIRONMENT

In this section we examine neutrino flavor transformation in the region above the neutrino sphere in models of post-core-bounce type II supernovae. There are several aspects of the problem of neutrino flavor transformation in supernovae which are significantly different from conventional computations of the MSW flavor conversion in the sun. Foremost among these is the necessity of treating the neutrino background. In addition, the geometry of neutrino emission from a neutrino sphere in a supernova is quite different from the solar case, where the neutrino source is distributed throughout the core.

Bearing these points in mind, we can formally transform the full flavor-basis Hamiltonian in Eqs. (17a) and (17b) to the basis of the instantaneous mass eigenstates $|\nu_1(t)\rangle$ and $|\nu_2(t)\rangle$. The Schrödinger equation for the time evolution of the amplitudes $a_{1\alpha}(t)$ and $a_{2\alpha}(t)$ [see Eq. (9)] in this basis is then

$$i\begin{pmatrix} \dot{a}_{1\alpha}(t) \\ \dot{a}_{2\alpha}(t) \end{pmatrix} = \begin{pmatrix} -\Delta_H(t)/2 & -i\dot{\theta}_H(t) \\ i\dot{\theta}_H(t) & \Delta_H(t)/2 \end{pmatrix}\begin{pmatrix} a_{1\alpha}(t) \\ a_{2\alpha}(t) \end{pmatrix} \ , \quad (23)$$

where $\dot{a}_{1\alpha}(t) = da_{1\alpha}(t)/dt$, $\dot{a}_{2\alpha}(t) = da_{2\alpha}(t)/dt$, and $\dot{\theta}_H(t) = d\theta_H(t)/dt$. In this expression we follow the treatment of neutrino propagation and flavor transformation in Ref. [8]. Equation (23) represents a set of *nonlinear* first-order differential equations for the amplitudes $a_{1\alpha}(t)$ and $a_{2\alpha}(t)$. The nonlinearity arises since, in general, Δ_H and the full effective mixing angle θ_H each depend on the neutrino background contributions B and $B_{e\tau}$ [Eqs. (19), (20a), and (20b)]. In turn, B and $B_{e\tau}$ depend on the amplitudes $a_{1\alpha}(t)$ as in Eqs. (22a) and (22b).

The time evolution of the full effective mixing angle can be found from Eqs. (20a) and (20b) to be

$$\dot{\theta}_H(t)$$

$$= \frac{\dot{B}_{e\tau}(\Delta\cos 2\theta - A - B) + (\Delta\sin 2\theta + B_{e\tau})(\dot{A} + \dot{B})}{2[(\Delta\cos 2\theta - A - B)^2 + (\Delta\sin 2\theta + B_{e\tau})^2]} , \tag{24}$$

where $\dot{A} = dA/dt$, $\dot{B} = dB/dt$, and $\dot{B}_{e\tau} = dB_{e\tau}/dt$.

We can define an "adiabaticity parameter" $\gamma(t)$:

$$\gamma(t) \equiv \frac{\Delta_H(t)}{2|\dot{\theta}_H(t)|} . \tag{25}$$

Clearly, the neutrino mass eigenstate evolution is well approximated as being adiabatic when $\gamma(t) \gg 1$. Of course, if $\dot{\theta}_H = 0$, the neutrino mass eigenstate evolution is completely adiabatic, as can be seen directly from Eq. (23).

The adiabaticity parameter generally satisfies $\gamma(t) \gg 1$ well away from resonance regions (neutrino mass-level-crossing regions). However, neutrino flavor conversion probabilities depend crucially on $\gamma(t)$ at resonance. We shall denote the value of the adiabaticity parameter at resonance as $\gamma(t_{\rm res})$. Resonance occurs when

$$\Delta\cos 2\theta = A + B . \tag{26}$$

We denote the position of this level-crossing point, or resonance, by $t_{\rm res}$. At resonance,

$$\gamma(t_{\rm res}) = \frac{(\Delta\sin 2\theta + B_{e\tau})^2}{|\dot{A} + \dot{B}|} = \frac{(\Delta\sin 2\theta + B_{e\tau})^2}{\Delta\cos 2\theta} \left| \frac{d\ln(A+B)}{dt} \right|^{-1}_{t_{\rm res}} . \tag{27}$$

So long as the approximation that the cross terms in the single neutrino density matrix are negligible is valid, the evolution of the mass eigenstates through the resonance region for a test neutrino can be described by the Landau-Zener formalism (cf. Ref. [8]). The Landau-Zener probability for the neutrino to jump from one mass eigenstate to the other in the course of transversing a resonance region is [8]

$$P_{\rm LZ} \approx \exp\left[-\frac{\pi}{2}\gamma(t_{\rm res})\right] . \tag{28}$$

Unlike the case for solar neutrinos, this expression is almost always sufficient for calculating neutrino flavor transformation in supernovae [5,6]. In fact, it is sufficient so long as we neglect the effects of the very small number of background neutrinos in the resonance region with nonzero density matrix element cross terms. The Landau-Zener formula Eq. (28) is inapplicable for solar neutrino flavor conversion when, for example, neutrinos are created close to their resonance positions. This never occurs in supernovae, where neutrinos originate on the neutrino sphere. The neutrino sphere is always well away from the resonance region for the cases we will consider. In addition, solar neutrinos can experience double level crossings when they are created at densities below their resonance density. This does not occur in the post-core-bounce supernova environment.

The very small vacuum mixing angles we shall consider for neutrino flavor conversion in supernovae imply narrow resonance regions. Narrow resonance regions, together with the generally large density scale heights (0.5–50 km) characteristic of the region above the neutrino sphere [5,6], imply that the first-order Landau-Zener jump probability expression in Eq. (28) is always adequate [5,6]. By "first-order" jump probability here, we mean that we approximate the density profile as linear across the resonance region.

It is obvious in Eqs. (24)–(27) that we recover the pure electron-driven neutrino flavor conversion case when the neutrino background disappears (i.e., B and $B_{e\tau}$ vanish everywhere). The neutrino background influences neutrino flavor evolution through resonances in two ways.

First, the diagonal contribution of the neutrino background, B, essentially shifts the position of the resonance from the case where only the electron contribution A is present. This is evident from Eq. (26). The diagonal contribution of the neutrino background also alters the density scale height of weak interaction scattering targets at resonance. The density scale height of weakly interacting targets $[|d\ln n/dr|^{-1}$ following Eq. (7) in Ref. [6]] is the $|d\ln(A+B)/dt|^{-1}$ term in Eq. (27).

The off-diagonal contribution of the neutrino background, $B_{e\tau}$, has the effect of altering the adiabaticity of the neutrino flavor evolution at resonance. This is clear from Eq. (27), where $B_{e\tau}$ appears in the expression for $\gamma(t_{\rm res})$. If $\Delta\sin 2\theta \gg |B_{e\tau}|$ then the off-diagonal neutrino background contribution will have little influence on the adiabaticity of neutrino flavor evolution.

However, the diagonal and off-diagonal contributions of the neutrino background influence neutrino flavor evolution in a nonlinear manner, as outlined above. Not only are B and $B_{e\tau}$ determined by the local neutrino distribution functions, but the local neutrino distribution functions are also dependent, in general, on the detailed history of neutrino flavor transformation.

The crux of the problem of treating the nonlinear effects of the neutrino background is the computation of B and $B_{e\tau}$ for the particular local neutrino distribution functions which obtain in the supernova environment. This will be evident if we discuss a simple iterative procedure for computing neutrino flavor transformation at resonance in the presence of a neutrino background.

We can employ the Landau-Zener transformation probability in Eq. (28) to estimate the neutrino flavor conversion probability for a neutrino propagating through a resonance with the following simple procedure. We choose a vacuum mass-squared difference δm^2 and a vacuum mixing angle θ (equivalently, $\sin^2 2\theta$) for a propagating neutrino of energy E_R.

(1) To begin with, we assume that $B_{e\tau} = 0$. We use δm^2 and $\sin^2 2\theta$, along with $B_{e\tau} = 0$, in Eqs. (20a) and (20b) to get a zero-order estimate for $\cos 2\theta_H$, $\sin 2\theta_H$, $\cos 2\bar{\theta}_H$, and $\sin 2\bar{\theta}_H$. Note that the value of A and

B which enter into the expressions for $\cos2\theta_H$, $\sin2\theta_H$, $\cos2\bar{\theta}_H$, and $\sin2\bar{\theta}_H$ are their values at the resonance position, $A(t_{\rm res})$ and $B(t_{\rm res})$. In this case we can replace $A+B$ by $(\delta m^2/2E_R)\cos2\theta$ wherever it occurs. Eqs. (20a) and (20b) with $B_{e\tau}=0$ can then be written as

$$\sin2\theta_H = \frac{\tan2\theta}{\sqrt{(1-E_\nu/E_R)^2+\tan^2 2\theta}} , \tag{29a}$$

$$\cos2\theta_H = \frac{1-E_\nu/E_R}{\sqrt{(1-E_\nu/E_R)^2+\tan^2 2\theta}} , \tag{29b}$$

$$\sin2\bar{\theta}_H = \frac{\tan2\theta}{\sqrt{(1+E_\nu/E_R)^2+\tan^2 2\theta}} , \tag{29c}$$

$$\cos2\bar{\theta}_H = \frac{1+E_\nu/E_R}{\sqrt{(1+E_\nu/E_R)^2+\tan^2 2\theta}} . \tag{29d}$$

(2) We employ these approximations for the full effective mixing angle to obtain estimates for B in Eq. (22a).

(3) So far we have not specified the resonance position. We now use A and the estimate of B from step (2) to estimate the resonance position through $(\delta m^2/2E_R)\cos2\theta = A+B$. Note that A and B are position dependent.

(4) With the resonance position from step (3) we use Eq. (22b) to estimate $B_{e\tau}$.

(5) With this estimate for $B_{e\tau}$ we now can reestimate the full effective mixing angle using

$$\sin2\theta_H = \frac{(\delta m^2/2E_\nu)\sin2\theta + B_{e\tau}}{\sqrt{[(\delta m^2/2E_\nu)-(\delta m^2/2E_R)]^2\cos^2 2\theta + [(\delta m^2/2E_\nu)\sin2\theta + B_{e\tau}]^2}} , \tag{30a}$$

$$\cos2\theta_H = \frac{[(\delta m^2/2E_\nu)-(\delta m^2/2E_R)]\cos2\theta}{\sqrt{[(\delta m^2/2E_\nu)-(\delta m^2/2E_R)]^2\cos^2 2\theta + [(\delta m^2/2E_\nu)\sin2\theta + B_{e\tau}]^2}} , \tag{30b}$$

$$\sin2\bar{\theta}_H = \frac{(\delta m^2/2E_\nu)\sin2\theta - B_{e\tau}}{\sqrt{[(\delta m^2/2E_\nu)+(\delta m^2/2E_R)]^2\cos^2 2\theta + [(\delta m^2/2E_\nu)\sin2\theta - B_{e\tau}]^2}} , \tag{30c}$$

$$\cos2\bar{\theta}_H = \frac{[(\delta m^2/2E_\nu)+(\delta m^2/2E_R)]\cos2\theta}{\sqrt{[(\delta m^2/2E_\nu)+(\delta m^2/2E_R)]^2\cos^2 2\theta + [(\delta m^2/2E_\nu)\sin2\theta - B_{e\tau}]^2}} . \tag{30d}$$

(6) We iterate by returning to step (2) and reevaluating B.

This procedure must be continued until $B, B_{e\tau}, \theta_H$, and the resonance position ($t_{\rm res}$) converge. Because of the dependence of B and $B_{e\tau}$ on the flavor evolution histories of all neutrinos in the ensemble, convergence of this procedure is, in general, problematic. However, if neutrino flavor evolution is adiabatic then the complication of prior histories is eliminated, and the above procedure converges rapidly for the conditions which obtain in the region above the neutrino sphere in type II supernovae. For nonadiabatic neutrino flavor evolution the above procedure, though more laborious, still gives good estimates of the effects of the neutrino background. We shall begin by discussing the case of adiabatic neutrino flavor evolution.

A. Adiabatic neutrino flavor evolution

Consider the flavor evolution of antineutrinos. It is generally true everywhere above the neutrino sphere that the contributions of the electrons and neutrinos satisfy $A+B>0$. This is true because n_e is everywhere greater than the net neutrino number densities for any neutrino flavor [5,6]. For an antineutrino emitted from the neutrino sphere in the $|\bar{\nu}_\alpha\rangle$ flavor eigenstate, it is evident that $|\bar{a}_{1e}(t)|^2 \approx 1$ and $|\bar{a}_{1\tau}(t)|^2 \approx 0$ for all t. The effective mass-squared difference for two antineutrino mass eigenstates always *increases* with density, and there is no mass level crossing. The adiabatic approximation for the evolution of the antineutrino mass eigenstates is always good.

The situation is more complicated for neutrinos. However, the approximation of adiabatic evolution of the neutrino mass eigenstates is a particularly simple case to treat in the supernova. A neutrino created in a flavor eigenstate $|\nu_\alpha\rangle$ at the neutrino sphere is very nearly in a mass eigenstate because of the large electron number density there. Subsequent adiabatic evolution then implies that, for example, $|a_{1e}(t)|^2 = 0$ and $|a_{1\tau}(t)|^2 = 1$ for all t (likewise, $|a_{2e}(t)|^2 = 1$ and $|a_{2\tau}(t)|^2 = 0$ for all t). In this case the expressions for the neutrino background contributions, Eqs. (22a) and (22b) become

$$B \approx -\sqrt{2}G_F \int (1-\cos\theta_{\mathbf{q}})[\cos2\theta_H(t)(dn_{\nu_e}-dn_{\nu_\tau}) + \cos2\bar{\theta}_H(t)(dn_{\bar{\nu}_e}-dn_{\bar{\nu}_\tau})] , \tag{31a}$$

$$B_{e\tau} \approx \sqrt{2}G_F \int (1-\cos\theta_{\mathbf{q}})[\sin2\theta_H(t)(dn_{\nu_e}-dn_{\nu_\tau}) + \sin2\bar{\theta}_H(t)(dn_{\bar{\nu}_e}-dn_{\bar{\nu}_\tau})] . \tag{31b}$$

The evaluation of Eqs. (31a) and (31b) for particular neutrino distribution functions is straightforward so long

as the adiabatic approximation obtains. To begin with, consider the computation of B from Eq. (31a) in the limit where $B_{e\tau}=0$. The result so obtained will be valid if we can later show that $|B_{e\tau}| \gg (\delta m^2/2E_R)\sin 2\theta$.

With the approximation that $B_{e\tau}$ is small the integrals over the neutrino distribution functions dn_{ν_e}, dn_{ν_τ}, $dn_{\bar{\nu}_e}$, and $dn_{\bar{\nu}_\tau}$ can be separated into an angular part and an energy part. This is due to the fact that when $B_{e\tau}$ is small θ_H and $\bar{\theta}_H$ essentially become functions of energy alone. For a radially propagating neutrino, the angular part of the integral in Eq. (31a) then becomes

$$\int (1-\cos\theta_{\mathbf{q}})\frac{d\Omega_{\mathbf{q}}}{4\pi} = \frac{1}{2}\int_0^{\theta_0}(1-\cos\theta_{\mathbf{q}})\sin\theta_{\mathbf{q}}\,d\theta_{\mathbf{q}} = \frac{1}{4}[1-\sqrt{1-(R_\nu/r)^2}]^2 \ . \tag{32a}$$

In this equation r is the radius of the point at which we evaluate B and θ_0 is the polar angle of the limb of the neutrino sphere as seen from this point. Frequently we are interested in regions sufficiently distant from the neutrino sphere that we can take $r \gg R_\nu$. In this limit, the radial neutrino path to the point at radius r is a good representation of all neutrino paths to that point, and we can approximate

$$\int (1-\cos\theta_{\mathbf{q}})\frac{d\Omega_{\mathbf{q}}}{4\pi} \approx \frac{1}{16}\frac{R_\nu^4}{r^4} \ . \tag{32b}$$

It is obvious from this expression that the diagonal contribution of the neutrino background is sensitive to position.

The integration of the remaining energy dependent terms in Eq. (31a) is simple if we employ the approximate energy spectra in Eq. (12c). The energy part of Eq. (31a) is then

$$\int \cos 2\theta_H f_{\nu_\alpha}(E_{\nu_\alpha})dE_{\nu_\alpha} \approx F_\nu(\theta, E_R/T_{\nu_\alpha}) \ , \tag{33a}$$

$$\int \cos 2\bar{\theta}_H f_{\bar{\nu}_\alpha}(E_{\bar{\nu}_\alpha})dE_{\bar{\nu}_\alpha} \approx F_{\bar{\nu}}(\theta, E_R/T_{\bar{\nu}_\alpha}) \ , \tag{33b}$$

where we define the neutrino spectral integrals as

$$F_\nu(\theta, x_R) \equiv \frac{1}{F_2(0)}\int_0^\infty \frac{1-x/x_R}{\sqrt{(1-x/x_R)^2+\tan^2 2\theta}}\frac{x^2}{\exp(x)+1}dx \ , \tag{34a}$$

$$F_{\bar{\nu}}(\theta, x_R) \equiv \frac{1}{F_2(0)}\int_0^\infty \frac{1+x/x_R}{\sqrt{(1+x/x_R)^2+\tan^2 2\theta}}\frac{x^2}{\exp(x)+1}dx \ . \tag{34b}$$

Clearly, for $\tan 2\theta \ll 1$, $F_{\bar{\nu}}(\theta, x_R) \approx 1$. Here E_R is the energy corresponding to a neutrino at resonance at radius r.

With these definitions, and for small $B_{e\tau}$, we can reduce Eq. (31a) for B to

$$B \approx -\sqrt{2}G_F\frac{[1-\sqrt{1-R_\nu^2/r^2}]^2}{4}[n^0_{\nu_e}F_\nu(\theta, E_R/T_{\nu_e}) - n^0_{\nu_\tau}F_\nu(\theta, E_R/T_{\nu_\tau}) + n^0_{\bar{\nu}_e}F_{\bar{\nu}}(\theta, E_R/T_{\bar{\nu}_e}) - n^0_{\bar{\nu}_\tau}F_{\bar{\nu}}(\theta, E_R/T_{\bar{\nu}_\tau})] \ , \tag{35}$$

where $n^0_{\nu_e}, n^0_{\nu_\tau}, n^0_{\bar{\nu}_e}$, and $n^0_{\bar{\nu}_\tau}$ are the appropriate neutrino or antineutrino number densities at the neutrino sphere as in Eq. (12b). This zero-order expression for B is to be used in step (2) in the iterative procedure outlined above. To proceed further requires that we estimate $B_{e\tau}$.

The angular integration for Eq. (31b) is the same as for Eq. (31a). In performing the angular integration in Eq. (31b) we will again assume that $B_{e\tau}$ is small. The energy dependent integrals in Eq. (31b) can be written as

$$\int \sin 2\theta_H f_{\nu_\alpha}(E_{\nu_\alpha})dE_{\nu_\alpha} \approx G_\nu(\theta, E_R/T_{\nu_\alpha}) \ , \tag{36a}$$

$$\int \sin 2\bar{\theta}_H f_{\bar{\nu}_\alpha}(E_{\bar{\nu}_\alpha})dE_{\bar{\nu}_\alpha} \approx G_{\bar{\nu}}(\theta, E_R/T_{\bar{\nu}_\alpha}) \ . \tag{36b}$$

In like manner to Eqs. (34a) and (34b) we define

$$G_\nu(\theta, x_R) \equiv \frac{1}{F_2(0)}\int_0^\infty \frac{\tan 2\theta}{\sqrt{(1-x/x_R)^2+\tan^2 2\theta}}\frac{x^2}{\exp(x)+1}dx \ , \tag{37a}$$

$$G_{\bar{\nu}}(\theta, x_R) \equiv \frac{1}{F_2(0)}\int_0^\infty \frac{\tan 2\theta}{\sqrt{(1+x/x_R)^2+\tan^2 2\theta}}\frac{x^2}{\exp(x)+1}dx \ , \tag{37b}$$

where the notation is as in Eqs. (34a) and (34b).

Finally, we can utilize Eqs. (36a)–(37b) to give an approximate expression for $B_{e\tau}$:

$$B_{e\tau} \approx \sqrt{2} G_F \frac{[1-\sqrt{1-R_\nu^2/r^2}]^2}{4} [n^0_{\nu_e} G_\nu(\theta, E_R/T_{\nu_e}) - n^0_{\nu_\tau} G_\nu(\theta, E_R/T_{\nu_\tau}) + n^0_{\bar{\nu}_e} G_{\bar{\nu}}(\theta, E_R/T_{\bar{\nu}_e}) - n^0_{\bar{\nu}_\tau} G_{\bar{\nu}}(\theta, E_R/T_{\bar{\nu}_\tau})] \ . \quad (38)$$

The notation in this equation is the same as in Eq. (35). The approximations for B and $B_{e\tau}$ in Eqs. (35) and (38), respectively, are valid when, $|B_{e\tau}|/(\delta m^2/2E_R)\sin 2\theta \ll 1$.

Note that the integrand in the expression for $G_\nu(\theta, x_R)$ in Eq. (37a) contains a factor, $\sin 2\theta_H \approx \tan 2\theta/\sqrt{(1-x/x_R)^2+\tan^2 2\theta} = \tan 2\theta/\sqrt{(1-E_\nu/E_R)^2+\tan^2 2\theta}$, which is sharply peaked at $E_\nu = E_R$ for small vacuum mixing angles. In Fig. 5 we plot $\sin 2\theta_H$ as a function of E_ν/E_R for three values of the vacuum mixing angle. The dotted line in this figure corresponds to $\tan 2\theta = 10^{-3}$. The dashed line corresponds to $\tan 2\theta = 10^{-2}$, while the solid line is for $\tan 2\theta = 0.1$. Since the factor $\sin 2\theta_H$ appears in the integration over the neutrino energy spectrum we can see easily that the smaller the vacuum mixing angle, the smaller will be the fraction of the total number density of neutrinos which contribute to $B_{e\tau}$. The physical interpretation of this is clear: the neutrinos which make the largest contribution to the off-diagonal neutrino background terms are those which have the largest full effective mixing angles at the position under consideration at radius r. These are the neutrinos which have energies close to E_R.

With the iterative procedure outlined above we can estimate B and $B_{e\tau}$ for adiabatic neutrino flavor evolution in both the shock reheating epoch and the hot bubble r-process nucleosynthesis epoch. References [5] and [6] give detailed expositions of the expected neutrino emission parameters for these epochs. Typical neutrino luminosities for the shock reheating epoch at $t_{\rm PB} \approx 0.15$ s (see the discussion in Ref. [5]) are $L_{\nu_e} \approx L_{\bar{\nu}_e} \approx L_{\nu_{\tau(\mu)}} \approx L_{\bar{\nu}_{\tau(\mu)}} \approx 5 \times 10^{52}$ erg s^{-1}. The neutrino sphere radius at this epoch is $R_\nu \approx 50$ km, while the average neutrino energies are $\langle E_{\nu_e}\rangle \approx 9$ MeV, $\langle E_{\bar{\nu}_e}\rangle \approx 12$ MeV, and $\langle E_{\nu_{\tau(\mu)}}\rangle \approx \langle E_{\bar{\nu}_{\tau(\mu)}}\rangle \approx 20$ MeV. By contrast, in the later hot bubble r-process nucleosynthesis epoch ($t_{\rm PB} \approx 5$ s) the neutrino luminosities are $L_{\nu_e} \approx L_{\bar{\nu}_e} \approx L_{\nu_{\tau(\mu)}} \approx L_{\bar{\nu}_{\tau(\mu)}} \approx 10^{51}$ erg s^{-1}, while the neutrino sphere is at radius $R_\nu \approx 10$ km. The average neutrino energies for this epoch are $\langle E_{\nu_e}\rangle \approx 11$ MeV, $\langle E_{\bar{\nu}_e}\rangle \approx 16$ MeV, and $\langle E_{\nu_{\tau(\mu)}}\rangle \approx \langle E_{\bar{\nu}_{\tau(\mu)}}\rangle \approx 25$ MeV.

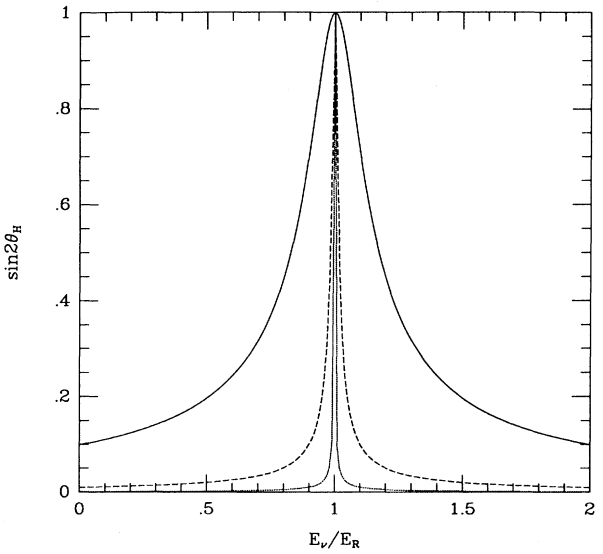

FIG. 5. The zero-order expression for $\sin 2\theta_H$ as a function of E_ν/E_R for three different vacuum mixing angles. The dotted line corresponds to $\tan 2\theta = 10^{-3}$. The dashed line corresponds to $\tan 2\theta = 10^{-2}$, while the solid line is for $\tan 2\theta = 0.1$.

As Ref. [5] shows, for a substantial enhancement in shock reheating ν_τ (or ν_μ) neutrinos with energies $E_\nu \approx 35$ MeV must be efficiently transformed into ν_e neutrinos in the region behind the stalled shock. Reference [6] shows that neutrinos with energies $E_\nu \approx 25$ MeV are the most important in determining the electron fraction, Y_e, in the hot bubble r-process nucleosynthesis epoch.

For shock reheating enhancement we *must* have adiabatic transformation of neutrinos with energies $E_\nu \approx 35$ MeV. In the hot bubble r-process nucleosynthesis epoch adiabatic transformation is not *necessary* to drive the material too proton rich for r-process nucleosynthesis to occur ($Y_e > 0.5$). In fact Ref. [6] shows that $\nu_{\tau(\mu)} \rightleftharpoons \nu_e$ flavor conversion efficiencies as small as $\sim 30\%$ for neutrinos with energies $E_\nu \approx 25$ MeV will suffice to drive $Y_e \geq 0.5$. Nevertheless, for large enough vacuum mixing angles, adiabatic transformation of neutrinos with $E_\nu \approx 25$ MeV will occur in some regions of the $(\delta m^2, \sin^2 2\theta)$ plot (Fig. 2 in Ref. [6]).

Consider adiabatic neutrino flavor conversion specifically for $E_\nu = 35$ MeV in the shock reheating epoch, and $E_\nu = 25$ MeV in the hot bubble r-process nucleosynthesis epoch. For comparison, we first present values of δm^2 and $\sin^2 2\theta$ which give an adiabaticity parameter $\gamma = 3$ for the bare electron number density distributions relevant for these epochs. In Figs. 6 and 7, the solid contour lines for $\gamma = 3$ correspond to these values of δm^2 and $\sin^2 2\theta$ for the representative conditions in the shock reheating and hot bubble r-process nucleosynthesis epochs, respectively.

It should be noted that the adiabatic approximation will be valid over the whole range of neutrino energies implicit in the neutrino distribution functions entering into the expressions for B and $B_{e\tau}$. Neutrinos with energies $E_\nu < E_R$ will propagate through resonances *prior* to reaching the resonance position for the specific example neutrino energy under discussion (either $E_R = 35$ MeV or $E_R = 25$ MeV). It is a general feature of the density scale height above the neutrino sphere that the neutrinos with energies $E_\nu < E_R$ will experience adiabatic flavor evolution through their resonances as long as neutrinos with energy E_R go through the resonance adiabatically [5,6]. Background neutrinos with energies $E_\nu > E_R$ will

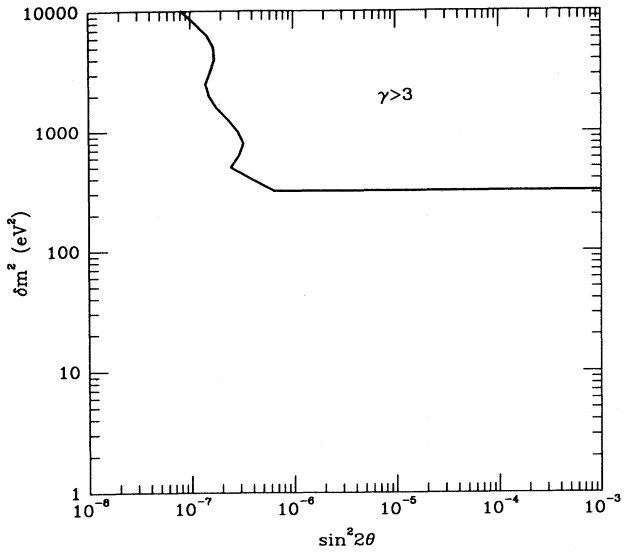

FIG. 6. Contour lines for $\gamma = 3$ on the $(\delta m^2, \sin^2 2\theta)$ plot for the shock reheating epoch. The solid contour line is calculated for the bare electron number density. The dotted line, which cannot be distinguished from the solid line in this case, is calculated with the neutrino background contributions.

not have gone through resonances and therefore evolve adiabatically *prior* to arriving at the resonance position for a neutrino with energy E_R. We conclude that the expressions for B and $B_{e\tau}$ in Eqs. (31a) and (31b) are appropriate for the example under consideration.

Using the iterative procedure outlined above we can calculate the true adiabatic parameter, $\gamma(t_{\rm res})$, including the neutrino background contributions. We show the new contour lines for $\gamma = 3$ as dotted lines in Figs. 6 and 7 for the respective epochs. We can easily see that the neutrino background has a completely negligible effect on adiabaticity at resonance along the solid $\gamma = 3$ contour line in Fig. 6. The new contour line for $\gamma = 3$ in Fig. 6 is indistinguishable from the one calculated for the bare electron number density. The new contour line for $\gamma = 3$ in Fig. 7 moves a little bit to the right of the solid line, but the neutrino background effects are also evidently small.

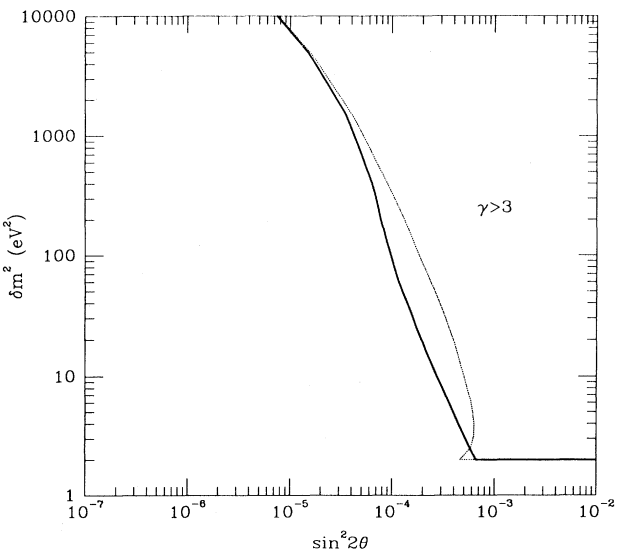

FIG. 7. As in Fig. 6, but for the hot bubble r-process nucleosynthesis epoch.

Any neutrino mixing parameters δm^2 and $\sin^2 2\theta$ which are to the right of the $\gamma = 3$ contour lines in Figs. 6 and 7 correspond to larger values of γ for the specific example neutrino energies under discussion. For a given δm^2 the ratio $|B_{e\tau}|/(\delta m^2/2E_R)\sin 2\theta$ will *decrease* as $\sin^2 2\theta$ and, hence, γ *increases*. The off-diagonal neutrino background contribution will have a negligible effect on neutrino flavor conversion everywhere to the right of the contour lines in Figs. 6 and 7. Likewise, B is roughly constant for a given δm^2 as $\sin^2 2\theta$ and, hence, γ is increased. The diagonal contribution of the neutrino background produces a negligible alteration in the computed flavor conversion efficiencies everywhere to the right of the contour lines in Figs. 6 and 7.

We have also examined adiabatic neutrino flavor conversion in supernovae for a range of neutrino energies. We can conclude that the neutrino background, specifically B and $B_{e\tau}$, will not result in any modification of the results of Refs. [5] and [6] whenever *adiabatic* neutrino flavor evolution is at issue.

B. Nonadiabatic neutrino flavor evolution

The effects of the neutrino background on nonadiabatic neutrino flavor evolution in the region above the neutrino sphere are potentially more significant than are the neutrino background effects on adiabatic neutrino flavor evolution. In general, the evaluation of B and $B_{e\tau}$ from Eqs. (22a) and (22b) is considerably more complicated when neutrino flavor evolution is nonadiabatic than it is when the adiabatic limit for neutrino flavor evolution obtains.

A neutrino of energy E_R, nonadiabatically going through a resonance at a point above the neutrino sphere, experiences a neutrino background effect which depends on the prior histories of all the neutrinos in the ensemble which are passing through the resonance region. As discussed above for this case, we cannot argue that background neutrinos with $E_\nu < E_R$ go through resonances adiabatically. The flavor evolution for background neutrinos with $E_\nu > E_R$ can still be considered adiabatic for the purposes of calculating B and $B_{e\tau}$, since these neutrinos will not yet have gone through resonances when they are in the resonance region for energy E_R.

In Fig. 8 we graphically illustrate the difficulties inherent in computing B and $B_{e\tau}$ from Eqs. (22a) and (22b) for nonadiabatic neutrino flavor evolution. In this figure we show the radial path of a neutrino with energy E_R. The resonance position for this neutrino is the point labeled RES(E_R). The path for a neutrino of energy E_B representative of the neutrino background at the point RES(E_R) is labeled by E_B. If $E_B < E_R$ then the neutrino on the path labeled by E_B presumably propa-

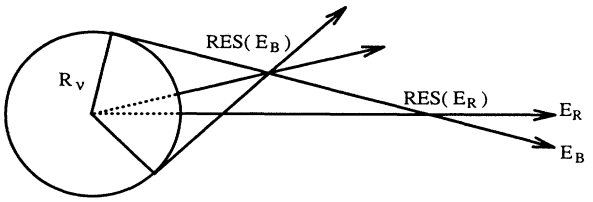

FIG. 8. Illustration of the difficulties inherent in computing the neutrino background contributions B and $B_{e\tau}$ for the case of nonadiabatic neutrino flavor evolution. The radial path of a neutrino with energy E_R and resonance position RES(E_R) is shown. The path for a neutrino of energy E_B representative of the neutrino background at position RES(E_R) is shown together with its resonance position RES(E_B). Paths for background neutrinos at position RES(E_B) are also shown.

gated through a resonance of its own prior to reaching position RES(E_R). The resonance position for the background neutrino is labeled RES(E_B). Whether or not this background neutrino experiences flavor conversion at RES(E_B) depends, in turn, on the flavor evolution histories of the background neutrinos which pass through this point. The paths for some of these "secondary" background neutrinos are shown in Fig. 8.

As we can see from Fig. 8, an exact calculation of the neutrino background contributions requires us to follow simultaneously the flavor evolution histories of neutrinos with different energies on all possible neutrino paths above the neutrino sphere. This could be done in a Monte Carlo calculation. However, there is a simpler alternative if we make note of the following two facts. First, we are most interested in regions which are far away from the neutrino sphere. The region for r-process nucleosynthesis in the hot bubble is located at radii $r > 4R_\nu$. So the polar angles for neutrino paths to a point in this region lie in a narrow range around $\theta_{\rm q} = 0$. In addition, at a point close to the neutrino sphere where the polar angles for the relevant neutrino paths can be significantly different from zero, the electron number density is so high that neutrino background effects can be safely ignored. Therefore, we can make an approximation and take the flavor evolution history of a radially propagating neutrino ($\theta_{\rm q} = 0$) as representative of the flavor evolution histories of all neutrinos with the same energy.

The flavor evolution history of radially propagating neutrinos for a given set of δm^2 and $\sin^2 2\theta$ can then be calculated with the following procedure:

(1′) We numerically represent the neutrino energy spectrum with a grid of energy bins. These energy bins cover a neutrino energy range of 1–100 MeV. Typically our numerical calculations employ $\sim$ 200 energy bins. Since neutrinos with lower energies go through resonances first, we start the calculations at the lower end of the energy grid.

(2′) For the particular grid point (neutrino energy bin) at neutrino energy E_ν, we use the iterative procedure outlined at the beginning of this section to locate the resonance position, $t_{\rm res}(E_\nu)$, for this particular neutrino energy E_ν. As a byproduct of this iterative procedure, we will obtain the corresponding neutrino background contributions B and $B_{e\tau}$ at this position $t_{\rm res}(E_\nu)$. The evaluation of B and $B_{e\tau}$ in this case is quite similar to that for the case of adiabatic neutrino flavor evolution, except that here we must use Eqs. (22a) and (22b) together with the flavor evolution histories of neutrinos with energies lower than E_ν.

(3′) Using the resonance position, $t_{\rm res}(E_\nu)$, and the corresponding neutrino background contributions B and $B_{e\tau}$ from step (2′), we can evaluate the Landau-Zener probability $P_{\rm LZ}(E_\nu)$ [Eq. (28)] for a neutrino with energy E_ν to jump from one mass eigenstate to the other in the course of transversing the resonance region. Now of course, it is in the use of the Landau-Zener jump probability for estimates of neutrino flavor conversion efficiency at resonance that we rely heavily on our approximation regarding the phases of background neutrinos at resonance. This approximation is that we can neglect the density matrix cross term effects of the very small number of background neutrinos in the resonant region defined by $E_\nu(1-\tan 2\theta)$ to $E_\nu(1+\tan 2\theta)$. We are confident from the arguments given above that this is a valid approximation for the supernova model parameters of Ref. [6]. But we must bear in mind that it may not be generally valid for other supernova environments or models—it must be checked on a case-by-case basis.

(4′) The flavor evolution history of ν_e neutrinos with energy E_ν is then approximated as

$$|a_{1e}(t)|^2 \approx \begin{cases} 0 & \text{if } t \le t_{\rm res}(E_\nu)\ , \\ P_{\rm LZ}(E_\nu) & \text{otherwise.} \end{cases} \tag{39}$$

Likewise, the flavor evolution history of ν_τ neutrinos with energy E_ν is approximated as

$$|a_{1\tau}(t)|^2 \approx \begin{cases} 1 & \text{if } t \le t_{\rm res}(E_\nu)\ , \\ 1 - P_{\rm LZ}(E_\nu) & \text{otherwise}\ . \end{cases} \tag{40}$$

In the above two equations, the evolutionary parameter t increases away from the neutrino sphere. These approximations for the neutrino flavor evolution history, together with Eqs. (22a) and (22b), are then used in the iterative procedure in step (2′) to locate the resonance position and calculate the corresponding neutrino background contributions for neutrinos with energies higher than E_ν.

At the end of the above procedure, we will have obtained the approximate flavor evolution histories for all the neutrino energies on the energy grid. This information then can be used to calculate the electron fraction Y_e in the r-process nucleosynthesis region as described in Ref. [6]. We present the new $Y_e = 0.5$ line, including the neutrino background effects, as a dotted contour line on the $(\delta m^2, \sin^2 2\theta)$ plot in Fig. 9. The original $Y_e = 0.5$ line in Fig. 2 of Ref. [6] is shown as the solid contour line in Fig. 9. To the right of the $Y_e = 0.5$ line, the material will be driven too proton rich for r-process nucleosynthesis to occur in the hot bubble.

By examining the two contour lines in Fig. 9, we can draw two conclusions. First, with a proper treatment of the neutrino background effects, we see that r-process nucleosynthesis in the hot bubble remains a sensitive probe of the flavor-mixing properties of neutrinos with

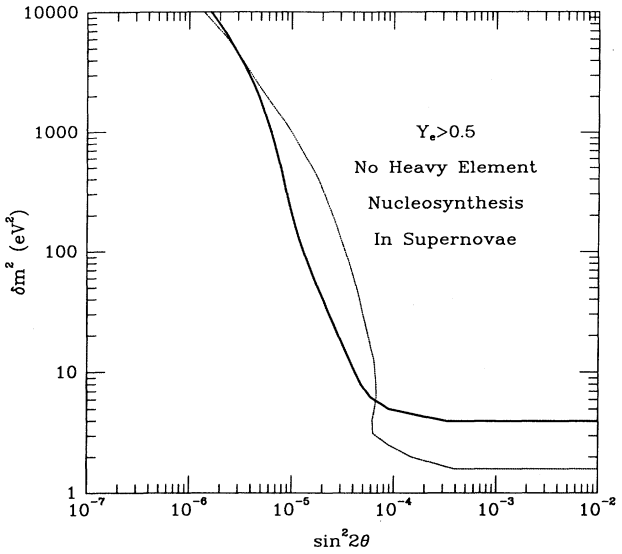

FIG. 9. Contour lines for $Y_e = 0.5$ are shown on the $(\delta m^2, \sin^2 2\theta)$ plot. The solid line is the same as the $Y_e = 0.5$ line in Fig. 2 of Ref. [6], whereas the dotted line is calculated with the full neutrino background contributions.

cosmologically significant masses. In fact, inclusion of the neutrino background contributions results in a small modification of the original $Y_e = 0.5$ line for $\delta m^2 = 4$ eV^2 to $\delta m^2 = 10^4$ eV^2. Furthermore, after we take into account the neutrino background contributions, it is evident that the range of neutrino vacuum mass-squared difference δm^2 probed by r-process nucleosynthesis is *extended* down to $\delta m^2 < 2$ eV^2. The reason for this extension can be found in the nonlinear nature of neutrino flavor transformation in the presence of a neutrino background.

Close to the neutrino sphere where little neutrino flavor transformation has occurred, the number density of ν_e neutrinos is larger than that of ν_τ neutrinos. This is because the luminosities for ν_e and ν_τ are approximately the same, but the average ν_τ neutrino energy is much higher [cf. Eq. (12b)]. However, with neutrino flavor transformation, more ν_e neutrinos are transformed into ν_τ neutrinos than ν_τ neutrinos are transformed into ν_e neutrinos. This is because there are more low energy ν_e neutrinos and only low energy neutrinos are very efficiently transformed for the parameters along the dotted contour line in Fig. 9. Because of the nonlinear evolution of the neutrino background, the diagonal contribution B evolves from a positive value for positions close to the neutrino sphere to a negative value for positions far away from the neutrino sphere. Neutrinos with $\delta m^2 < 2$ eV^2 and energies over a broad range will tend to have resonances far enough out that the diagonal contributions will satisfy $B < 0$. For a given δm^2 and a given energy E_ν, the resonance position will lie closer to the neutrino sphere for the case $B < 0$ than it would for the case where no neutrino background is present [cf. Eq. (26)].

As Ref. [6] discusses, Y_e and r-process nucleosynthesis are sensitive to neutrino flavor conversion only when resonances occur inside the weak freeze-out radius. The weak freeze-out radius is the radius beyond which typical ν_e and $\bar{\nu}_e$ capture rates are small compared to the material expansion rate. When $B < 0$, the resonance positions for given δm^2 are drawn in toward the neutrino sphere. Hence, we find that the $Y_e = 0.5$ line drops to lower values of δm^2 in the presence of a neutrino background.

Clearly, these results depend on the assumption that $\nu_{\tau(\mu)}$ is the heavier neutrino species. Were this not the case, then matter-enhanced flavor transformation only occurs in the antineutrino sector. Conclusions regarding the effects of neutrino background would be different in that case.

IV. CONCLUSIONS

We have calculated neutrino flavor transformation in the region above the neutrino sphere in type II supernovae including all contributions from the neutrino background. In particular, we have examined the neutrino background effects on both cases of adiabatic and nonadiabatic neutrino flavor evolution. In the case of adiabatic neutrino flavor evolution, which is most relevant for supernova shock reheating, we find that the neutrino background has a completely negligible effect on the range of vacuum mass-squared difference δm^2 and vacuum mixing angle θ or equivalently $\sin^2 2\theta$, required for enhanced shock heating. In the case of nonadiabatic neutrino flavor evolution relevant for r-process nucleosynthesis in the hot bubble, we find that r-process nucleosynthesis from neutrino-heated supernova ejecta remains a sensitive probe of the mixing between a light ν_e and a $\nu_{\tau(\mu)}$ with a cosmologically significant mass. The modification of the $(\delta m^2, \sin^2 2\theta)$ parameter region probed by r-process nucleosynthesis due to the neutrino background effects is generally small. The nonlinear nature of neutrino flavor transformation in the presence of a neutrino background actually *extends* the sensitivity of r-process nucleosynthesis to smaller values of δm^2.

In general, we find that a proper account of neutrino background effects leads to no modification in the overall qualitative conclusions of Refs. [5] and [6]. At the early epochs of the post-core-bounce supernova environment ($t_{\rm PB} < 1$ s), we find that the characteristically large electron number densities and large density scale heights determine the phenomenon of neutrino flavor transformation.

Even at the later epochs associated with r-process nucleosynthesis, the effects of the neutrino background on neutrino flavor evolution are small. In fact, the neutrino background does produce a decrease relative to Ref. [6] in the sensitivity of r-process nucleosynthesis to the vacuum mixing angle for $\nu_{\tau(\mu)} \rightleftharpoons \nu_e$ when $\delta m^2 < 3000$ eV^2. This decrease in sensitivity, as measured by the position of the $Y_e = 0.5$ line, is at most a factor of 3 in $\sin^2 2\theta$. Most of the effect on Y_e near the $Y_e = 0.5$ line in this case, however, comes from *nonadiabatic* neutrino flavor conversion, $\nu_{\tau(\mu)} \rightleftharpoons \nu_e$. Of course, we have presented only an approximate treatment of the neutrino background for the case of nonadiabatic neutrino flavor evolution, in that we have

neglected the phase effects of the small number of background neutrinos in which path length differences from the resonance sphere or energy distribution averaging are not effective in reducing the cross terms in ensemble averages. We have argued that the phase effects of these background neutrinos are negligible simply because they represent only a very small fraction of the total number of background neutrinos at a given point.

In contrast, these phase issues are completely absent and irrelevant for the case where neutrino flavor evolution is adiabatic. In this sense, the "adiabatic-limit" $Y_e > 0.5$ line in Fig. 7 represents an overly conservative limit on the effects of neutrino mixing on r-process nucleosynthesis.

What about the effects of uncertainties in the supernova models on our conclusions? It is in general not straightforward to answer this question, though our feeling is that these uncertainties are relatively small, especially as regards the r-process nucleosynthesis epoch of supernova evolution. Such uncertainties are addressed in Refs. [5,6]. In this paper, we have presented neutrino flavor evolution calculations employing the parameters of the best available supernova model for r-process nucleosynthesis [6].

Reference [6] discusses the uncertainties of these model calculations and their impact on any conclusions regarding neutrino flavor evolution. There it was emphasized that r-process nucleosynthesis takes place *long after* the chaotic and uncertain supernova-explosion epoch where the shock is reenergized. As such, the r-process epoch is characterized by quiescent neutrino-heated outflow, and there are three readily identifiable parameters: the entropy, the outflow velocity, and the neutrino luminosity. The latter two parameters essentially determine the position of the weak freeze-out radius [6] and so determine the position of the lower horizontal line in Figs. 7 and 9. Increasing the neutrino luminosity would have the effect of increasing all neutrino background effects at a given radius.

For example, increasing the neutrino luminosity in the context of the Ref. [6] model would have the effect of pushing the horizontal $Y_e = 0.5$ line (lowest δm^2 sensitivity) to even lower values, while at the same time pushing the diagonal part of this line to larger $\sin^2 2\theta$. However, it is not at all obvious that such a sensitivity study makes sense at this point. Increasing the neutrino luminosities or the material outflow velocities, or otherwise changing the model parameters of Ref. [6], would probably have the effect of ruining the excellent agreement between the computed r-process abundance yields and the observed solar system distribution of the r-process elements [9,10]. Only time will tell if the hot bubble environment is truly the site of r-process, though this seems highly likely given the results of Ref. [10].

ACKNOWLEDGMENTS

We want to thank J. R. Wilson and R. W. Mayle for much patient education on the subject of supernova neutrinos. We would like to acknowledge discussions with A. B. Balantekin and W. C. Haxton. Y.-Z. Qian also acknowledges discussions with M. Herrmann and M. Burkardt. This work was supported by the Department of Energy under Grant No. DE-FG06-90ER40561 at the Institute for Nuclear Theory and by NSF Grant No. PHY-9121623 and an IGPP minigrant at UCSD.

[1] G. Sigl and G. Raffelt, Nucl. Phys. **B406**, 423 (1993).
[2] S. Samuel, Phys. Rev. D **48**, 1462 (1993).
[3] G. M. Fuller, R. W. Mayle, J. R. Wilson, and D. N. Schramm, Astrophys. J. **322**, 795 (1987).
[4] D. Nötzold and G. Raffelt, Nucl. Phys. **B307**, 924 (1988).
[5] G. M. Fuller, R. W. Mayle, B. S. Meyer, and J. R. Wilson, Astrophys. J. **389**, 517 (1992).
[6] Y.-Z. Qian, G. M. Fuller, G. J. Mathews, R. W. Mayle, J. R. Wilson, and S. E. Woosley, Phys. Rev. Lett. **71**, 1965 (1993).
[7] L. Wolfenstein, Phys. Rev. D **17**, 2369 (1978); **20**, 2634 (1979); S. P. Mikheyev and A. Yu. Smirnov, Nuovo Cimento Soc. Ital. Fis. **9C**, 17 (1986); H. A. Bethe, Phys. Rev. Lett. **56**, 1305 (1986).
[8] W. C. Haxton, Phys. Rev. D **36**, 2283 (1987).
[9] B. S. Meyer, G. J. Mathews, W. M. Howard, S. E. Woosley, and R. Hoffman, Astrophys. J. **399**, 656 (1992).
[10] S. E. Woosley, G. J. Mathews, J. R. Wilson, R. Hoffman, and B. S. Meyer, Astrophys. J. **433**, 229 (1994).